

Electronic Supplementary Information:

Control of pressure-driven components in integrated microfluidic devices using an on-chip electrostatic microvalve

Joshua D. Tice,^a Amit V. Desai,^a Thomas A. Bassett,^a Christopher A. Apblett^{*b,c}
and Paul J.A. Kenis^{*a}

^a *Department of Chemical & Biomolecular Engineering, University of Illinois at Urbana-Champaign, 600 South Mathews Avenue, Urbana, IL 61801, USA. Tel: 1 217 265 0523; E-mail: kenis@illinois.edu*

^b *Sandia National Laboratories, Albuquerque, NM 87185, USA. Tel: 1 505 844 3497; E-mail: caapble@sandia.gov*

^c *Department of Chemical & Nuclear Engineering, University of New Mexico, Albuquerque, NM 87131, USA.*

Fabrication

We fabricated the electrostatic microvalve using only soft-lithographic techniques (See Fig. 5 in main text). Molds for channels and microvalve chambers were made by patterning SU-8 5 photoresist (Microchem Corp.) with standard photolithographic techniques onto silicon wafers. For channels 2 μm tall, the photoresist was spun at 7,200 rpm for 30 s, and for channels 7 μm tall, the photoresist was spun at 1,700 rpm for 30 s. For some of the molds, we added SU-8 posts to form through-holes for the electrostatic microvalves. To form the posts, SU-8 50 was spin-coated on top of the previously formed features at 1,500 rpm for 30 s and then processed according to the manufacturer's specifications. Molds for the support layer were fabricated using either SU-8 50 (spun at 2000 rpm for 30 s) or SU-8 5 (spun at 3000 rpm for 30 s). Molds for the stamps were fabricated using SU-8 50 spun at 2000 rpm for 30 s. To reduce adhesion between poly(dimethylsiloxane) and the molds, a surface treatment was performed by placing the molds in a vacuum desiccator along with several drops of (tridecafluoro-1,1,2,2-tetrahydrooctyl)trichlorosilane (Gelest, Inc.) and then applying vacuum overnight.

To form electrodes of multi-walled carbon nanotubes (MWNTs) (Fig. 5a), an aqueous suspension of MWNTs (20-30 nm outer diameter, 10-30 μm length, > 95 wt% purity, ash < 1.5 wt%, Cheaptubes, Inc.) with a ratio of 1 mg MWNTs : 10 mg sodium dodecyl sulfate : 1 mL deionized water was prepared and sonicated with a probe (Vibra-Cell VCX130PB, Sonics & Materials, Inc.) for approximately 30 min to solubilize the MWNT. A 0.5-1 mL sample was then diluted into approximately 20-30 mL deionized water and stirred briefly. The dilute suspension was filtered through a membrane filter (Anodisc™ inorganic membrane, 0.1 or 0.2 μm pore size, 47 mm diameter, Whatman) that had been wet with ethanol. After the aqueous suspension had fully passed through the membrane, the MWNT that remained on the membrane were washed with ethanol until the filtrate was free of bubbles.

To construct the upper layers of the microvalve (Fig. 5b), a thin layer of PDMS (20 monomer : 1 curing agent weight ratio, General Electric RTV 615, Hisco, Inc.) was first spin-coated onto the mold at 10,000 rpm for 300 s (for 2 μm tall channels) or 50 s (for 7 μm tall channels) such that a thin film covered the channel features but not the SU-8 posts for the through-holes. The PDMS film was cured in an oven at 70 °C for 1 h and then allowed to cool to room temperature. A PDMS stamp (20 monomer : 1 curing agent weight ratio, cured overnight at 70 °C) was brought into contact with the MWNT film. Areas in contact with the stamp were lifted off the membrane filter and then applied to the PDMS film formed previously. Pressure was applied by hand, and after lifting off the PDMS stamp, a fraction of the MWNT film transferred to the PDMS film. The transparency of the MWNT film allowed us to perform alignment in a straightforward manner. (Characterization of the MWNT electrodes and the transfer printing process appear elsewhere.)¹⁻² Electrical contacts were made from a mixture of PDMS (5 monomer : 1 curing agent weight ratio) and 10 wt% MWNTs, which was applied at two corners of the

MWNT film and subsequently cured for 15 min in an oven at 70 °C. To encapsulate the MWNT electrode, a second layer of PDMS (20 monomer : 1 curing agent weight ratio) was spin-coated on top of the electrode at 3000 rpm for 30 s and allowed to cure until tacky in an oven at 70 °C for 20-30 min. The PDMS support layer (5 monomer : 1 curing agent weight ratio; cured at 70 °C for 1 h) was aligned onto the membrane; uncovered regions of the spin-coated PDMS layers were filled with liquid PDMS (5 monomer : 1 curing agent weight ratio), and the whole assembly was cured overnight in an oven at 70 °C. The support layer sealed permanently to the membrane due to the mismatch of curing agent concentration between the layers. The upper layers of the microvalve were removed from the mold and holes were punched to the inlets of the microchannels using a sharpened 20 gauge steel needle. If through-holes were not formed previously by means of SU-8 posts incorporated into the molds, the through-holes were cut with a scalpel or sharpened needle.

To fabricate the lower electrode for the microvalve (Fig. 5c), a featureless silicon wafer was treated with silane vapor as described previously, and a thin layer of PDMS (20 monomer : 1 curing agent weight ratio), diluted in hexanes (10 hexanes : 1 PDMS weight ratio) was spin-coated onto the wafer at 10,000 rpm for 120 s. The thin PDMS layer was cured in an oven at 70 °C for 1 h, and then a MWNT film was applied as described above. Electrical contacts were also applied, and the wafer was then covered with a layer of PDMS (5 monomer : 1 curing agent weight ratio) several millimeters thick. The PDMS was cured overnight at 70 °C.

To integrate a pneumatic microvalve into the layer containing the lower electrode, the fabrication was modified as follows. After spin-coating a thin layer of PDMS, transferring the MWNT film, and applying the electrical contacts, we spin-coated a second layer of PDMS (20 monomer : 1 curing agent weight ratio) at 2400 rpm for 30 s. The PDMS was cured at 70 °C for

20-30 min until slightly tacky, and then another layer of PDMS (5 monomer : 1 curing agent weight ratio; cured at 70 °C for at least 1 h) with a rounded microchannel was aligned and placed on top. Uncovered regions of the spin-coated PDMS layers were filled with liquid PDMS (5 monomer : 1 curing agent weight ratio) and the whole assembly was cured overnight at 70 °C. The mold for the rounded microchannel channel was made by spin-coating Microposit™ SPR220™-7 photoresist at 1,500 rpm for 60 s (10 µm thick). The remainder of the photoresist processing was performed according to the manufacturer's specifications. Following development, the mold was heated at 150 °C for 30 min. to allow the resist to reflow, which created a rounded cross-section.

To seal the upper layers of the microvalve to the lower electrode (Fig. 5d), both surfaces participating in the seal were exposed to oxygen plasma generated with an atmospheric plasma system (Atomflo™ 400L system equipped with an AH-250L head, Surfx Technologies). The system was configured to 100 W RF power, with an oxygen flow rate of 0.03 L min⁻¹ and a helium flow rate of 15.0 L min⁻¹. The bonding surfaces were passed under the nozzle of the plasma system by hand at approximately 2 cm s⁻¹. After waiting 20 min., they were aligned and brought into contact. During the sealing process, the membrane was reversibly laminated to the top of the pressure-balancing channel to prevent unwanted collapse of the membrane onto the floor of the microvalve chamber. After the bond was completed, the membrane was delaminated by pressurizing the channels. To complete the seal, the device was heated at 70 °C for at least 1 h.

Determination of valve dimensions

To determine critical valve dimensions, valves were cut in half to expose the cross-sections and then observed with a scanning electron microscope (JEOL 6060LV SEM). Channel depths were measured with a profilometer (Dektak 3030). Lateral dimensions were measured with an optical stereoscope (Leica M025 C).

Characterization of actuation potentials and isolation pressures

To characterize the actuation potentials of the electrostatic microvalves, we first filled fluidic control channels with fluorinated oil (3M™ Fluorinert™ FC-40) and sealed the outlet of the control channel by purposefully not punching an access hole during fabrication. The inlet of the control channel was attached to a vial filled with fluorinated oil and attached to a source of pressurized nitrogen *via* a pressure controller (Cole Parmer, model 68027-78). Leads from a DC power supply (Hewlett Packard model 6209B) were attached to wires which were inserted into the electrical contacts made of PDMS and MWNTs, with the upper electrode negatively polarized. While applying a constant pressure to the inlet, the potential was increased slowly until the microvalve shut. After shutting, the potential was increased further and micrographs were taken through a stereoscope (Leica M025 C) to quantify the area of the membrane that was in contact with the channel floor.

To characterize the response of the membrane to increasing pressures at a fixed potential, we attached the inlet to a regulated nitrogen tank, actuated the microvalve at a low pressure, and then used the regulator to slowly increase pressure until the membrane released from the channel floor. Micrographs were also taken to quantify the area of the membrane that was in contact with the channel floor.

Characterization of pressures generated by pressure amplifier circuits

A pressure sensor, consisting of a membrane suspended above a microfluidic chamber in fluidic communication with the control channel, was integrated into the pressure amplifier circuit during fabrication. The outlet of the microfluidic circuit was shut with a piece of Teflon® tubing that was filled with cured PDMS. A calibration curve was derived by increasing the pressure in increments of 5 kPa, and collecting images of the pressure sensor through a stereoscope. The images were then analyzed with digital photo processing software.

To characterize the pressures that could be generated with the microfluidic pressure amplifier circuits, the outlet was opened, and the electrostatic microvalve was actuated at a given potential. An image of the pressure sensor was again collected and compared with the calibration curve to extract a reading.

Failure mode testing

A microvalve with a chamber height of 2 μm and a diameter of 400 μm was cycled at 0.2 Hz while applying a pressure of 40-60 kPa. The potential was generated with a custom-designed electrical circuit that produced a square-wave signal with a peak-to-peak voltage of 250 V.

Finite element analysis of structure deformation due to pressurization

The effects of pressurization on structure deformation were investigated with a finite element analysis package, COMSOL Multiphysics®, utilizing the solid mechanics module. Material properties of PDMS were assigned the values in the following table:

Property	Value
Young's modulus, membrane	4.0 MPa
Young's modulus, bulk	1.5 MPa
Poisson's ratio	0.49
Density	965 kg m ⁻³

The PDMS was treated as an incompressible, linear elastic material, and we neglected any effect of embedded carbon nanotubes on material stiffening. Others have shown that the Young's modulus of PDMS is affected by the ratio of base polymer to cross-linking agent³ as well as the thickness of the PDMS layer³⁻⁴. Hence, different moduli were used for the PDMS in the membrane (bulk) and the PDMS in the support layer and lower layer of the device (bulk).

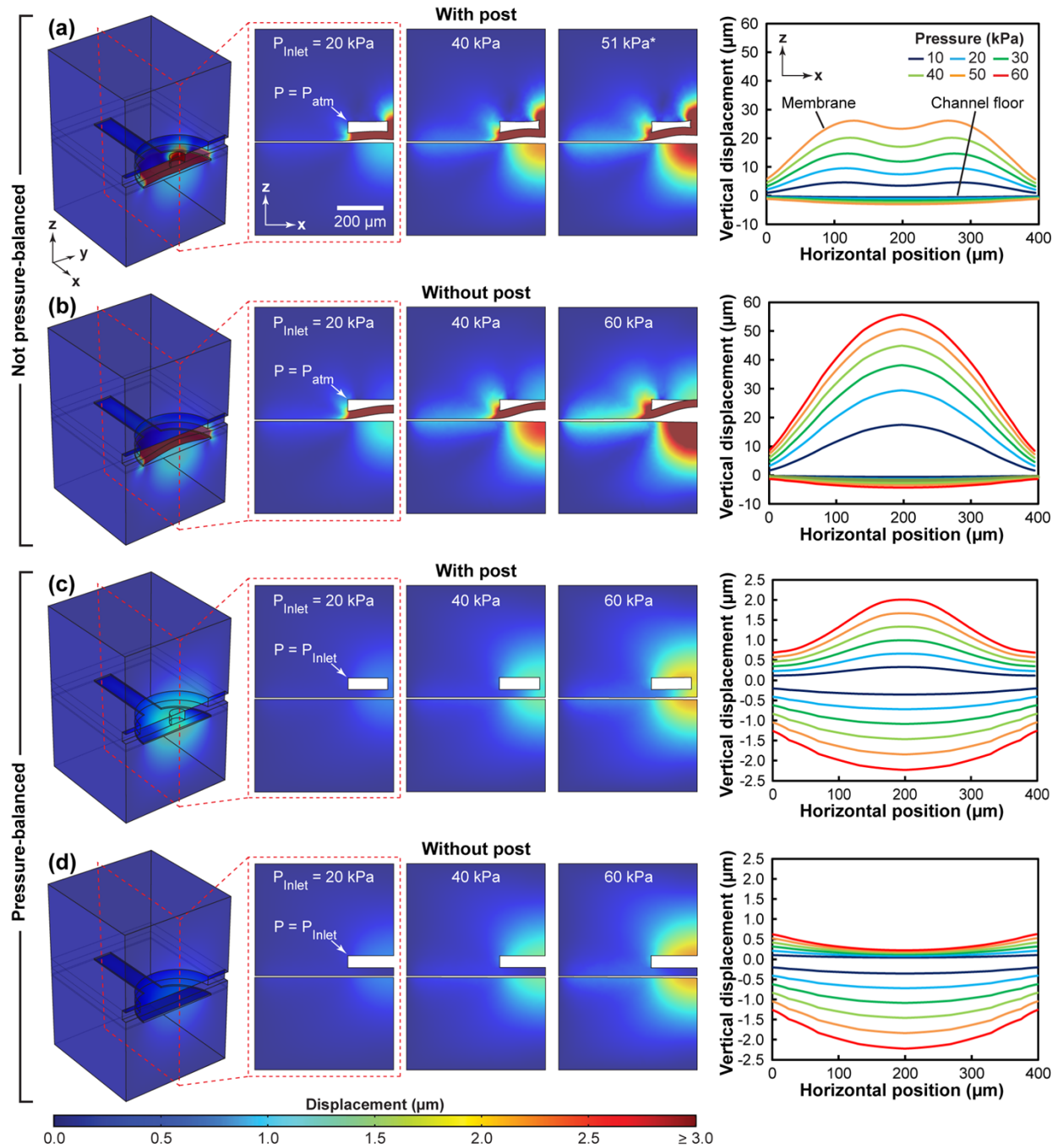


Fig. S1 Simulations of the effect of pressurization on different actuator configurations using a finite element method. (a-b) Simulation results for actuators where pressure was applied only in the main channel. (c-d) Simulation results for actuators where pressure was applied both in the main channel and in the venting channel. The actuators contained posts in the recess above the membrane for (a) and (c). The posts were omitted in (b) and (d). The graphs shown on the right depict the deflection of the membrane and the floor of the channel in the x-z plane that passes through the center of the actuator. Note that the scale of the y-axis differs between the graphs in (a-b) and the graphs in (c-d).

Model of the effect of ‘leakage channel’ dimensions on the fluidic resistance of the electrostatic microvalve

The hydraulic resistance of a rigid channel segment, $R_{h,segment}$, with rectangular cross-section, can be described with:⁵

$$R_{h,segment} = \frac{12\eta L_{segment}}{wh^3 \left(1 - \frac{h}{w} \left(\frac{192}{\pi^5} \sum_{n=1,3,5}^{\infty} \frac{1}{n^5} \tanh\left(\frac{n\pi w}{2h}\right) \right) \right)}, \quad (6)$$

where η is the dynamic viscosity of the hydraulic fluid, $L_{segment}$ is the length of the channel segment, w is the width of the channel, and h is the height of the channel.

When the electrostatic microvalve is closed, typically two narrow ‘leakage channels’ form around the periphery of the valve chamber due to the rectangular nature of the chamber’s cross section (Fig. 1c). These leakage channels contribute additional finite hydraulic resistance, $R_{h,valve}$, to the microfluidic circuit, which is incorporated in to eqns. (4) and (5) of the main text. To approximate $R_{h,valve}$, we assume the leakage channels have a rectangular cross-section, $(a - b)$ by h , and length πa (half the microvalve circumference) (See Fig. 4c of the main text). The two parallel leakage channels then have a combined hydraulic resistance of

$$R_{h,valve} = \frac{6\eta\pi a}{(a - b)h^3 \left(1 - \frac{h}{(a - b)} \left(\frac{192}{\pi^5} \sum_{n=1,3,5}^{\infty} \frac{1}{n^5} \tanh\left(\frac{n\pi(a - b)}{2h}\right) \right) \right)}. \quad (7)$$

To approximate the degree of closure needed for the electrostatic microvalve to be effective, we used eqns. (4) – (5), (7) to plot the expected P_{out} / P_{inlet} for different values of b/a with diameters, $2a$, between 200 – 400 μm . The model showed that b/a would have to be at least 0.96 (and in some cases > 0.99) to achieve more than 90% of P_{inlet} for the microfluidic buffer or less than 10% of P_{inlet} for the microfluidic inverter (Fig. S2).

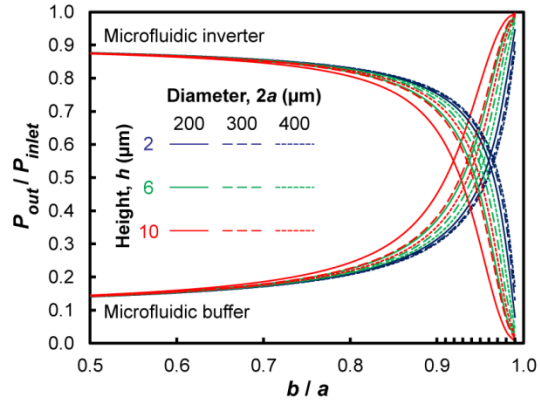


Fig. S2 A graph of the simulated expected pressure output of microfluidic pressure amplifier circuits as a function of the dimensions of the leakage channels of the electrostatic microvalve.

Supplementary references

- 1 J. D. Tice, T. A. Bassett, A. V. Desai, C. A. Apblett and P. J. A. Kenis, *Sensors and Actuators A: Physical*, 2013, **196**, 22-29.
- 2 J. Salzbrenner, C. Apblett and T. Khraishi, *Polym. Int.*, 2013, **62**, 608-615.
- 3 M. Liu and Q. Chen, *Journal of Micro/Nanolithography, MEMS and MOEMS*, 2007, **6**, 023008.
- 4 M. Liu, J. R. Sun, Y. Sun, C. Bock and Q. F. Chen, *J. Micromech. Microeng.*, 2009, **19**.
- 5 R. J. Cornish, *Proceedings of the Royal Society of London. Series A*, 1928, **120**, 691-700.